

ESTIMATING INTRINSIC ACCURACY OF AIRBORNE LASER DATA WITH LOCAL 3D-OFFSETS

Frédéric Bretar^a, Marc Pierrot-Deseilligny^a, Michel Roux^b

^a Institut Géographique National

2-4 Av. Pasteur 94165 St. Mandé cedex, France

Email: {Frederic.Bretar, Marc.Pierrot-Deseilligny}@ign.fr

^b GET-Télécom Paris - URA 820 LTCI - Département TSI

46 Rue Barrault 75013 Paris, France

Email: Michel.Roux@enst.fr

KEY WORDS: lidar, accuracy, local corrections, 3D-accumulators, deformation field, registration

ABSTRACT:

Airborne laser systems provide a three-dimensional (3D) perception of the Earth's topography with clouds of points. Whereas the technique ensures a high theoretical quality, one can observe discrepancies in certain areas. This situation may be of importance in case of joint sensor application, like merging airborne laser scanner with photogrammetry. The first step of a fusion process is to define a common reference frame so that a global geometric coherence should be extracted. This article describes a methodology for matching a single laser strip with a photogrammetric derived Digital Elevation Model (DEM), and as a result estimating intra-strip errors. It is based on calculating local linear deformations with a tri-dimensionnal accumulator (translation space). We show that searching for local discrepancy is equivalent to compute the maximum of the accumulator. 2D and 3D simulated problems are discussed in details and solved over known transformed data set. Results on real data show a significant improvement when applying retrieved local translations to laser points. After correction, both data sets tend to be expressed in the same reference frame. The accurate registration is then ensured.

1 INTRODUCTION

Laser altimetry has become an accurate technique to describe topography from an airborne platform. Initially, it provides a 3D cloud of points acquired by means of laser distance measurements, combined with an integrated GPS/ INertial System (Kilian et al., 1996). Due to the performances of the laser system to derive Digital Elevation Model (DEM), studies on laser accuracy focused onto height component. Huising (Huising and Pereira, 1998) in a detailed examination of the height accuracy potential of airborne laser-scanning, identifies a number of systematic errors. In order to provide a high density data set and to minimize occlusions, a laser data set consists of many parallel strips, which may overlap, with a width of several hundred meters. As a result, the fusion of several laser strips has been the crux of research focus for the past few years (Burman, 2000). Maas (Maas, 2002) proposed a method based on least-square matching on a TIN structure, which aims to estimate laser strip discrepancies in all three coordinate directions using both height and reflectance data on overlapped areas. Vosselman (Vosselman, 2002) uses the same methodology on height data but introduces an edge response function to enhance the estimation and increase the number of offset measurements between the strips.

However, errors introduced by the GPS/INS measurements cause systematic deformations of laser-scanner data strips. These effects may be of local nature, but may also cause shifts, tilts, or torsions of whole strip (Crombaghs et al., 2000). Nevertheless, theoretical predictions did not always explain errors in the final data set. In case of joint sensor applications, eg. merging airborne laser with photogrammetry, planimetric discrepancies have to be determined in order to work in a common reference frame. In this respect, Schenk (Schenk et al., 2001) presented a study of laser points accuracy which is based on comparing elevations and features in aerial images with their counter parts in the laser point cloud. He described a procedure where laser points are projected back to aerial images. He compared then the back-projected laser points with the corresponding gray values that represent the true surface. He mentioned that this methodology was not consis-

tent for estimating horizontal accuracy because linear features can hardly be directly retrieved from laser points.

In order to avoid the search for specific structures, we used a statistical approach. This study takes place in a global strategy for coupling both laser and photogrammetric data. The fusion of several sensors needs to work in a common reference frame. The aim of this article is to estimate 3D discrepancies between two data sets that are meant to represent the same topography. We will consider at first a single strip and analyze discrepancies within this strip.

In the first part of this paper, we enlighten the phenomena of local discrepancy between laser points and a DEM, followed by the description of our data sets (Section 3). We explain then our global strategy in Section 4 where the general algorithm is described. The two dimensional case and the 3D case are successively analyzed in details over simulated data in Section 4.2 and 4.3. The results of some experiments over raw laser data in urban areas are presented afterward in Section 5. Finally, we conclude this paper with future directions of our research.

2 BACKGROUND

Even if airborne laser data have a good intrinsic accuracy, it has been detected several mismatching problems when superimposing with a photogrammetric derived DEM. Figure 1 shows a visual discrepancy between the laser cloud of points represented with its typical point distribution and the triangulated DEM. The shaded surface represents a polygonal approximation of the DEM projected in the 3D object space superimposed onto the laser cloud of points. It is visible that both data sets are not exactly in the same geometric framework with a local offset of the laser points with regard to the DEM.

The final accuracy of both systems does not depend on the same parameters (that is why they may be used jointly). The DEM planimetric accuracy derives from the quality of image orientations (parameters of the point of view) and the altimetric component strongly depends on the correlation process. As

far as the laser data are concerned, errors were probably due to GPS/INS measurements, and especially to their acquisition frequency which is from far less than the laser pulse ones. It entails interpolations and related compensating calculations.

We aim to estimate *a posteriori* the accuracy of laser data with regard to a DEM using exclusively range measurements in order to perform an accurate co-registration of both data sets. This stage is a crucial step, for it determines the final accuracy of the projections that enter in the forthcoming fusion process. Our strat-

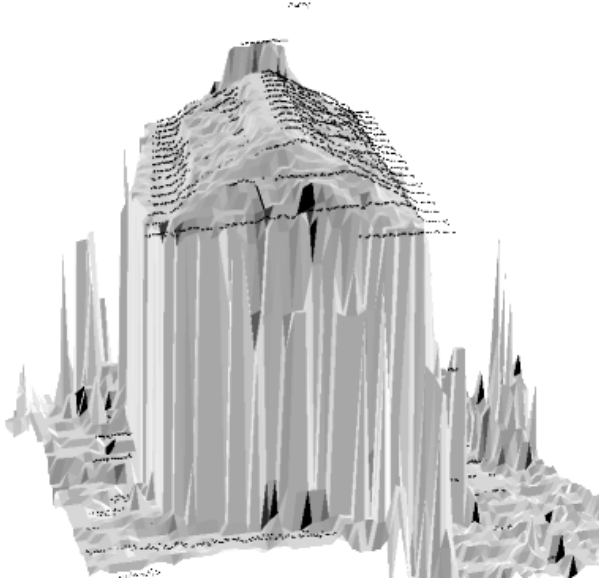


Figure 1: Superimposing shaded DEM (in gray) and **raw** 3D laser points (black points) over a building in the inner city of Amiens, France.

egy consists of determining local translations in order to estimate global deformations of the whole laser strip. In this paper, we are looking for small corrections, assuming that laser data and the DEM are approximatively well-referenced. As a result, the search space is limited on purpose at a translation of 5 meters, which is large compared to real deformations.

3 THE DATA SETS

We used in this study two sorts of data acquired at two different dates. This remark may be of importance because the topography may have changed in the mean time, entailing as a result artifacts in the accumulation process described in Section 4.

3.1 The Laser Data

The laser data set has been acquired over the city of Amiens, France, by TopoSys©. This firm owns a self-made lidar acquisition system, which is composed of two rigid blocks of optical fibers (emission and reception of laser pulses). Table 1 gathers the main technical information about the system.

The scan mechanism of TopoSys© is not based on a swiveling mirror but on a fixed glass fiber array. Its specific design produces a push-broom measurement pattern on the ground. The glass fiber scanner avoids positioning inaccuracies which may occur in case of a swiveling mirror in such a vibrating environment like an aircraft.

The spatial density is roughly one point every 10cm following the flight heading and one point every 1.2m in the cross-direction. It

Height Flight	1005 m
Strip Width	≈ 230 m
Scanning Frequency	650 Hz
Pulse Length	5 ns
Acquisition Frequency	83 kHz
Laser Wave Length	$1.55\mu\text{m}$
FOV	14°

Table 1: Technical characteristics of the TopoSys© lidar system.

is an average of $7.5 \text{ points}/\text{m}^2$. We will use a single strip for testing, since the strip adjustment problem is not considered in this article.

3.2 The DEM

The DEM used as a reference is calculated from correlation techniques using dynamic programming (Baillard, 1997) along epipolar lines. The final reliable DEM with 0.2m-resolution results from the fusion of a set of DEMs calculated from some pairs of images. The global geometric accuracy is guaranteed by the knowledge of the orientation of the set of aerial images. If we consider moreover that a DEM calculated from aerial imageries is sensitive to radiometric artifacts, we may tolerate a remaining noise, especially in the less-visible parts like narrow streets (in a urban context). That is the reason why a RMS criterion will not be used to quantify the enhancement of the algorithm applied to raw laser data, since the improvement would not be significant enough.

4 THEORETICAL CONSIDERATIONS

We have already seen that even though laser points and the DEM are meant to describe the same surface, they will not perfectly fit because of the different acquisition systems. The DEM is noisier than the laser point set because of the matching problems of correlation (see Section 3), without however altering the geometric coherence. Generally speaking, the algorithm consists of minimising the distance (least-square minimisation) between both clouds of points that represent the same topography. At a local scale, we try to fit both surfaces, under the hypothesis that the local movement is a translation. We describe in Section 4.1 the measurements of local translations.

4.1 Measurements of local translations

The algorithm developed in this study is based on calculating a linear approximation of the deformation field from local translations. In order to characterize these local 3D-offsets, we follow a statistical approach based on searching for the maximum of a 3D-accumulator, which represents the 3D-translation space (see Section 4.2 for justification). Accumulators presented in the following are cut at a constant t_z (figure 5(a), 5(b), 8(a), 8(b)).

Description of the algorithm Let us consider a set of adjacent square regions R (Equation 1), and the set L_R of laser points included in R (Equation 2).

$$R = [x_1, x_2] * [y_1, y_2] \in \mathbb{R}^2 \quad (1)$$

$$L_R = \{l_i = \begin{pmatrix} x_i \\ y_i \\ z_i \end{pmatrix} \}_{i \in \mathbb{N}}^{laser} / \begin{pmatrix} x_i \\ y_i \end{pmatrix} \in R \quad (2)$$

V_{l_i} is a neighborhood of DEM points centered onto the planimetric coordinates of a laser point l_i , and is explicitly written in

Equation 3, where C is the dimension of the neighborhood.

$$V_{l_i} = \left\{ p_j = \begin{pmatrix} x_j \\ y_j \\ z_j \end{pmatrix}_{j \in \mathbb{N}} \in DEM / \left\{ \begin{array}{l} |x_i - x_j| \leq C \\ |y_i - y_j| \leq C \end{array} \right\} \right\} \quad (3)$$

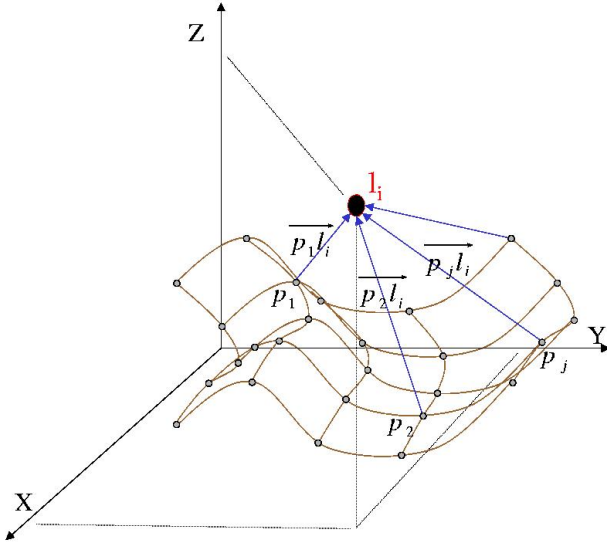


Figure 2: Diagram of the local accumulation process. The point l_i corresponds to the laser point in geographic coordinates, the gray points p_i are the nodes of the reference DEM.

The accumulation process consists of two main steps: at first, calculating a 3D accumulator with votes for specific translations. This stage is illustrated on Figure 2. For each laser point l_i and each neighborhood $V_{l_i} \in DEM$, we calculate the vector $\vec{p_j l_i}$, which is associated to a vote in the 3D-accumulator. Since the accumulator is not continuous, and seeing that the surface is noisy, we consider the vote not to be punctual, but gaussian. It means that each vote will influence its neighbors. We may show that convolving each vote independently by a gaussian is equivalent to a global convolution by the same gaussian. This filtering will smooth the accumulator surface and will make the maximum enhance (we will see that it is not always the case). Secondly, we look for the global maximum (the proof is given in Section 4.2).

Synthetic view of the algorithm The final algorithm can be described as follows:

- ```

0. For Each regions R
 Initiate the 3D accumulator array H
1. For Each laser point $l_i \in L_R$
 Compute a neighborhood V_{l_i} of DEM points
2. For each $p_j \in V_{l_i}$
 $\vec{p_j l_i} \in \mathbb{R}^3$
 $H(\vec{p_j l_i}) + 1$
 Endfor p_j
 Endfor l_i
3. Convolve H by a Gaussian filter
4. Search for global maximum in H
 Endfor R
5. Correct the laser cloud of points by $\{M_R\}_R$

```

We will analyze in details in Section 4.2 the 2D case with simulated data. In the mean time, we will prove that step 4 of the algorithm yields the local retrieved translation.

#### 4.2 The simulated 2D case

Let us consider  $K$  couples of points  $(x_k, f(x_k))$  where  $f$  is a function that describes the simulated topography (black profile in Figure 3). This data set will be taken as the reference DEM. We apply next a translation  $\begin{pmatrix} t_x \\ t_y \end{pmatrix}$  to this profile and build the  $L_R$  set of translated topographic points (gray profile in Figure 3).

$$L_R = \{l_k\}_{k \in [1, K]} = \{(x_k + t_x, f(x_k) + t_y)\}$$

$V_{l_i}$  is the set of  $n$  neighboring points of  $l_i$  in the reference set with  $i \in [1, K]$  and  $n \ll K$ :

$$V_{l_i} = \{p_j \in [1, n]\} = \{(x_1, f(x_1)), \dots, (x_n, f(x_n))\}$$

It follows that

$$\bigcap_{l_i \in L_R} \{\vec{p_j l_i} / p_j \in V_{l_i}\} = \vec{p_i l_i} = \begin{pmatrix} t_x \\ t_y \end{pmatrix}$$

$$\text{but } \forall i, j \in [1, K], i \neq j \quad H(\vec{p_i l_i}) > H(\vec{p_i l_j})$$

$$\text{therefore } \arg \max_{X \in \mathbb{R}^2} H(\vec{X}) = \vec{p_i l_i} = \begin{pmatrix} t_x \\ t_y \end{pmatrix} \quad (4)$$

Equation 4 ends up the proof that searching for the maximum of  $H$  leads to retrieve the applied translation. Figure 3(a) shows in black the reference profile, and the translated one in gray. The accumulator is also presented in gray level scale in Figure 3(b). The argument of the global maximum is the initial translation.

#### 4.3 Validation on 3D simulated data

The proof we gave in Section 4.2 can be easily extended in 3D considering local translations. In this section, we apply our algorithm over known 3D-transformed cloud of points, and analyze the final deformation field. We took as input data the sub-sampled DEM. The cloud of points is then transformed, and we apply the local accumulation algorithm to retrieve the deformation field.

**Description of the simulation** We decide to apply a rotation given by Equation 5

$$P' = R_1(\theta)R_2(\psi)R_3(\phi) \cdot P \quad (5)$$

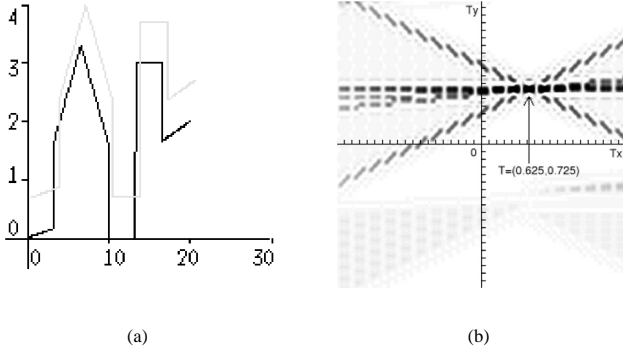


Figure 3: (a) Profiles representing the simulated topography (in black), and the translated one to be retrieved (in gray). The nominal translation is  $(0.6, 0.7)$  cm. (b) Related accumulator that indicates a maximum for  $(0.625, 0.725)$  cm. The final accuracy depends on the sampling step of the parameter space.

where  $R_1(\theta)$ ,  $R_2(\psi)$ ,  $R_3(\phi)$  are the  $3 \times 3$ -rotation matrix in the pitch, roll and yaw directions,  $P$  is the original 3D-point and  $P'$  the rotated 3D-point.

Results of the accumulation over the simulated situation are presented in Figure 4. One can point out that local translations globally fit well with the general movement. In order to quantify the validity of local translations, we used the RMS criterion which is defined in Equation 6, where  $z_{Corrected\ 3D\ Point \rightarrow DEM}$  is the DEM-related altimetry of the projection of the local corrected 3D-point.

$$RMS = \sqrt{\frac{\sum (z_{Corrected\ 3D\ Point \rightarrow DEM} - z_{DEM})^2}{n}} \quad (6)$$

We found that local corrections enhance the RMS of a factor 3. Seeing that the final RMS takes into account only linear approximations of the rotation, it is understandable that a bias remains.

By looking through the accumulators, it is possible to have a better understanding of the parameter space. In a urban environment, most of accumulators have a shape as presented in Figure 5(a) top. As one can notice it, we are performing the accumulation over orthogonal building edges (see Section 5). The strong multi-directional topographic gradient helps the accumulator to catch the desired solution. The global maximum is well-defined, without any ambiguity.

It may occur that the area whereupon the accumulation takes place does not fit these criteria. In such a case, we are in the situation shown in Figure 5(b). Here, the accumulator is blurred in each direction entailing a high inaccuracy for estimating the translation due to the flat topography of the DEM. There is an invariance with regard to planimetric translations. Such cases are observed in Figure 4 where the algorithm sometimes failed to retrieve the associated translation. Actually, the algorithm will always find a maximum in the accumulator. But it may not be reliable. In order to detect such configurations, we applied a threshold on the retrieved translation module. Above this value, the translation is not considered.

## 5 EXPERIMENTAL RESULTS AND DISCUSSION

### 5.1 Parameters of the algorithm

Results presented hereafter have been computed with the following parameters: the resolution of the accumulator is 0.1m in each

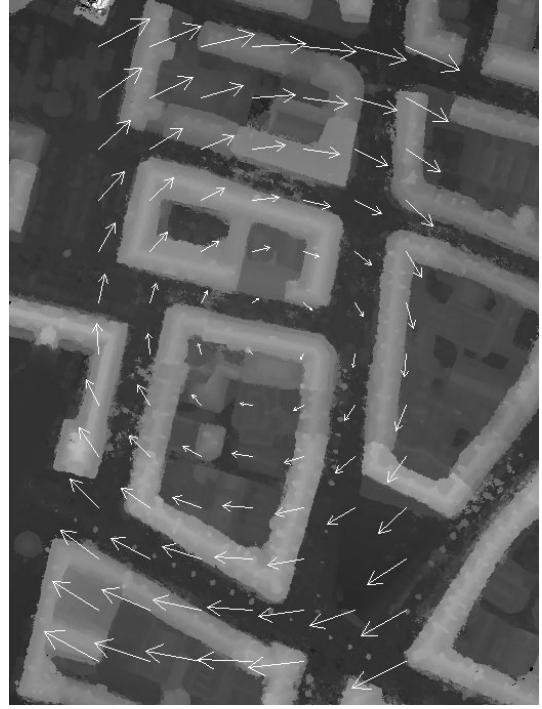


Figure 4: White arrows represent the deformation field computed from a rotated cloud of points. It is projected onto the DEM used as a reference in the accumulation process. In this simulation,  $\phi = 2^\circ$ ,  $\psi = 0^\circ$ ,  $\theta = 0^\circ$ , that is a rotation in the (X,Y) plane. For convenience, arrows are scaled with a factor 5.

component. It is filtered with a Gaussian convolution of standard deviation  $\sigma = 0.2\sqrt{2}m$ . We extracted adjacent laser point squares  $R$  of  $20 \times 20m^2$ , which include about 3000 laser points ( $card(L_R) \approx 3000$ ). The accumulation is made with respect to a partial DEM  $V_i$  of  $121 \times 121$  pixels, that is  $24.2 \times 24.2m^2$  with a 0.2m-resolution. As mentioned in Section 4.3, we introduce a threshold to limit the module of the translation at  $2m$ . For exhaustive exploration concern, the algorithm looks for translations included between  $-5m$  and  $+5m$  in each direction.

### 5.2 Results

Figure 6 depicts the same wire-frame as in Figure 1 but the laser data are corrected from the retrieved translation. Both data sets are more coherent than previously. One can note that laser points that are invisible on this picture are just below the wire-frame surface. We present on Figure 7 the results of local accumulations over a partial strip of 1.2km-length. This deformation field was calculated by blocks of around 300 000 laser points for RAM managing concern. We remark that certain parts of the strip are without any measurements. This situation is similar to the one described in Section 4.3, and many accumulators behave like in Figure 5(b). In case of a unidirectional topographic gradient, that is invariance by means of translations through a privileged direction like presented in Figure 8(a), it makes the uncertainty larger during the search for maxima, and at the end a false estimation of the translation. A more ideal case is shown on Figure 8(b) where the contributions of the building orthogonal directions distinguish a global sharp maximum. In this situation, the uncertainty is weak.

For a more complete description, Figure 9 shows two profiles of both raw laser data (in black) and the related DEM (in gray) over the same building. As it has already been mentioned, it exists a

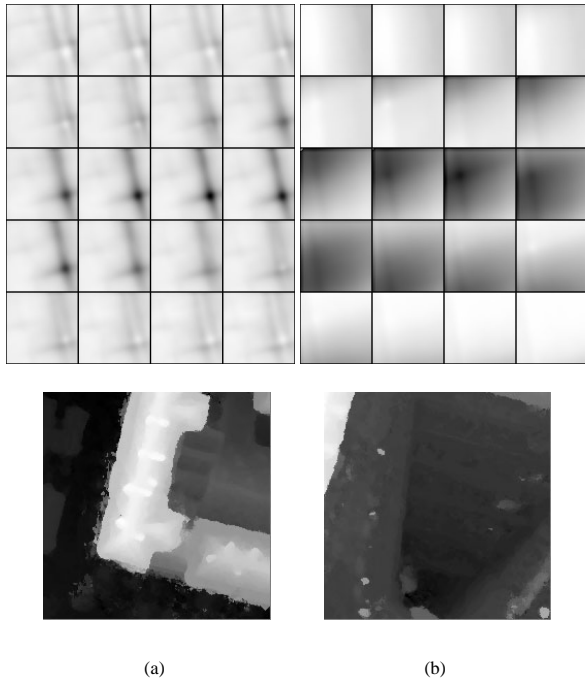


Figure 5: Top: Two accumulators volumes (slice by slice) calculated from a simulated case. The corresponding extracted DEM are shown underneath. (a) ideal case with high relief surface, (b) flat terrain entailing a blurred accumulator.

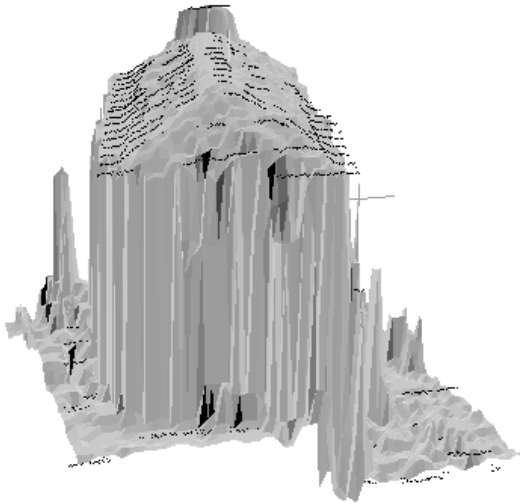


Figure 6: Wire-frame of the DEM superimposed onto the **corrected** laser points in black

remaining offset (top) between black points and the gray ones. One can notice on the second picture (bottom) that the laser data set is well-corrected with regard to the DEM. It is especially visible on the roof top. The value of the correction is in that case  $\begin{pmatrix} 0.35 \\ -0.35 \\ 0.05 \end{pmatrix}$  meter.

### 5.3 Discussion and futur work

The methodology presented in this paper is a statistical way to fit two surfaces. The main objective is less to quantify exactly the accuracy of laser data than having both data sets into the same geometry. We decided to use the photogrammetric derived DEM

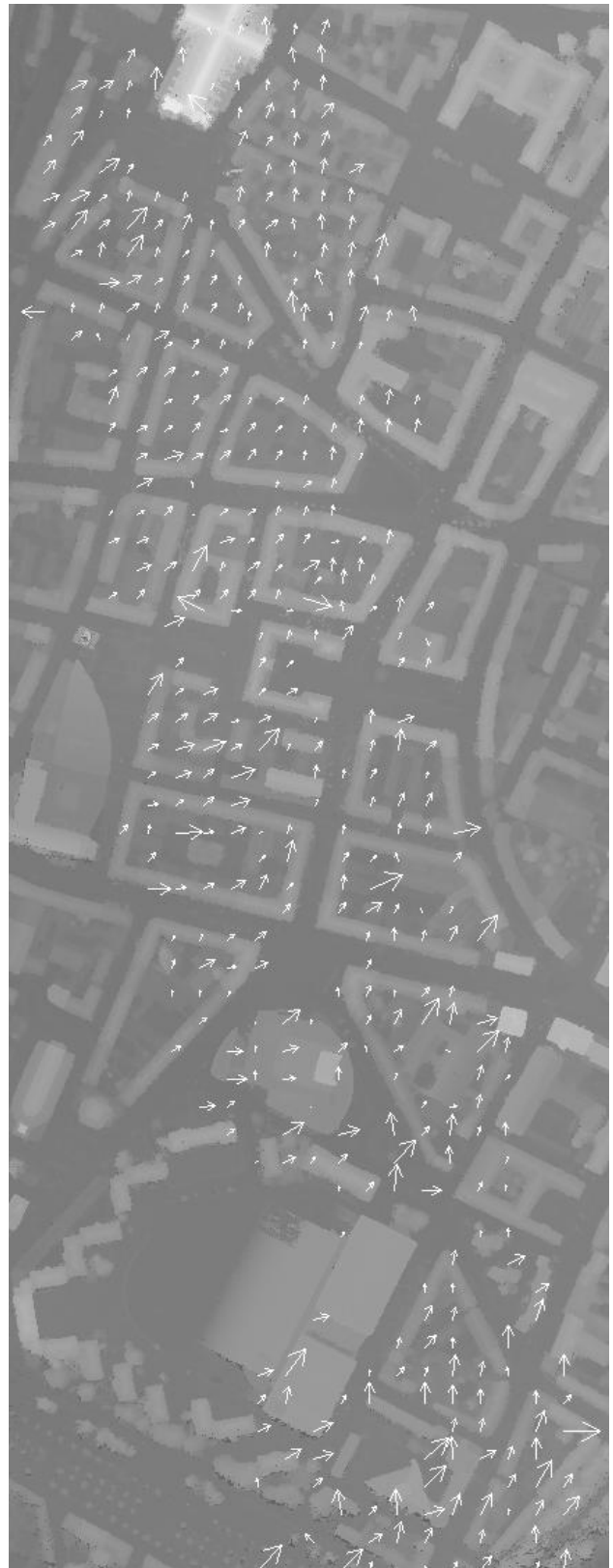


Figure 7: White arrows represent the local offset (planimetric component) of the laser data with respect to the DEM. For visibility, arrows are scaled with a factor 10.

as a reference, but this choice is subjective. Our method is reflexive, and it is possible to swap the laser data and the DEM. In a

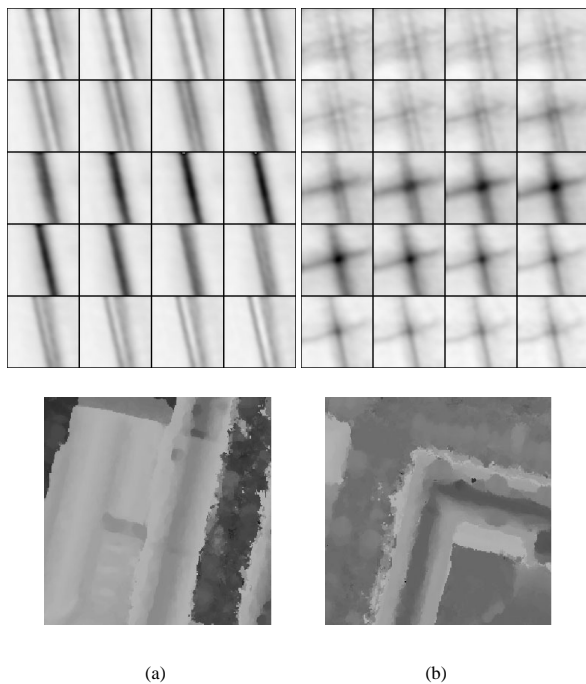


Figure 8: Top: Two accumulator volumes (slice by slice) calculated from raw laser data. The corresponding extracted DEM are shown underneath. (a) unidirectional accumulator leading to an inaccuracy in the search for maximum, (b) well-determined case.

fusion process, the aim is to work in a common reference frame, whatever technique be the best-georeferenced.

We did mention that the accumulator's shape was of importance for retrieving translations. We may analyse the inertial axis of the accumulators, and derive a reliability factor to quantify the correctness of the measurements. Several alternatives can be studied to enhance the accumulator's shape:

- enlarging the DEM neighborhood so that the DEM should contain more different landscapes, but the computing time will be drastically higher
- enlarging the laser neighborhood whereupon the accumulation takes place, but it is of importance to keep the local aspect of the estimation. We must find a trade-off between this local aspect and the multi-directional topography represented by the laser points
- since the algorithm is likely to fail in open areas with smooth/flat surfaces and along linear objects, it is conceivable to study these elements independently from the DEM and to apply a specific treatment.

At the time of the study, laser data are corrected by paving, what entails discontinuities at the paving edges. In this respect, considering the global deformation field shown in Figure 7, it is highly conceivable to derive a global continuous correction model. This model could be affine (12 parameters) or similar to a rigid movement (rotation - 9 parameters). Different estimation methods can be used to solve the system  $AX = B$ , especially the theory of M-estimators which deals with outliers (Xu and Zhang, 1996), and may be adequate to our problem.

There is no quantitative considerations for the improvement of the registration. We planned to develop a criterion to measure this improvement, like a correlation coefficient over profiles, or more generally, a 2D-correlation over a entire building.

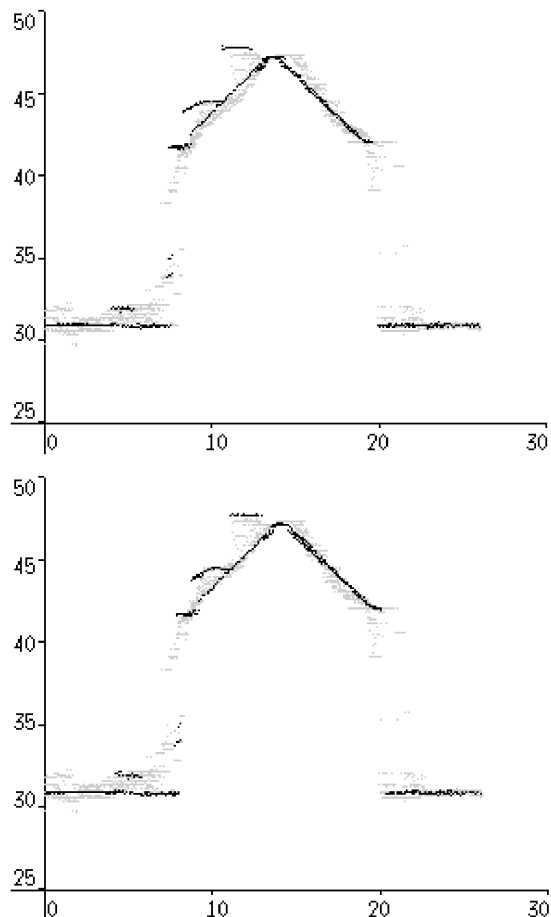


Figure 9: Profiles through a house scaled in meters. Top: profiles of both **raw** laser data (in black) and DEM (in gray). Bottom: profiles of both **corrected** laser data and DEM.

We would like to test the algorithm with different sorts of data (various landscapes and point density).

## 6 CONCLUSION

This paper presents a methodology for evaluating and correcting airborne laser data with regard to a photogrammetric derived DEM through a registration process. This process consists of calculating a local 3D-accumulator and estimating local 3D translations over a laser strip. The final results are two data sets into the same geometry that can be used jointly. The values of the correction may be of importance whether we work with high resolution images, especially when projecting into the image space. The final accuracy will therefore be optimal.

## REFERENCES

- Baillard, C., 1997. Analyse d'images aériennes stéréoscopiques pour la restitution 3D des milieux urbains. PhD thesis, École Nationale Supérieure des Télécommunications de Paris.
- Burman, H., 2000. Adjustment of laserscanner data for correction of orientation errors. Vol. XXXIII-3/W4, International Archives of Photogrammetry and Remote Sensing, pp. 125–132, Part B3/1.
- Crombaghs, M., R.Brugelmann and de Min, E., 2000. On the adjustment of overlapping strips of laseraltimeter height data. Vol. XXXIII, International Archives of Photogrammetry and Remote Sensing, pp. 224–231, Part B3/1.

Huising, E. and Pereira, L. G., 1998. Errors and accuracy estimates of laser data acquired by various laser scanning systems for topographic applications. *ISPRS Journal of Photogrammetry and Remote Sensing* 53 (5), pp. 245–261.

Kilian, J., Haala, N. and Englich, M., 1996. Capture and evaluation of airborne laser scanner data. Vol. XXXI, *International Archives of Photogrammetry and Remote Sensing*, pp. 383–388, Part B3.

Maas, H.-G., 2002. Method for measuring height and planimetry discrepancies in airborne laserscanner data. *Photogrammetric Engineering and Remote Sensing* 68(9), pp. 933–940.

Schenk, T., Seo, S. and Csatho, B., 2001. Accuracy study of airborne laser scanning data with photogrammetry. Vol. XXXIV-3/W4, *International Archives of Photogrammetry and Remote Sensing*.

Vosselman, G., 2002. On estimation of planimetric offsets in laser altimetry data. Vol. XXXIV, *International Archives of Photogrammetry and Remote Sensing*, Graz, Austria, pp. 375–380, Part A3.

Xu, G. and Zhang, Z., 1996. *Epipolar Geometry in stereo, motion and object recognition*. Kluwer Academic Publishers.